



Wet STEM: A new development in environmental SEM for imaging nano-objects included in a liquid phase

A. Bogner^{a,b,*}, G. Thollet^a, D. Basset^b, P.-H. Jouneau^a, C. Gauthier^a

^a*Groupe d'Etudes de Métallurgie Physique et de Physique des Matériaux, UMR CNRS 5510, INSA de Lyon, Bâtiment B. Pascal, 7 Avenue Jean Capelle, 69 621 Villeurbanne Cedex, France*

^b*Total France, Centre de Recherche de Solaize, BP 22 69360 Solaize Cedex, France*

Received 20 August 2004; received in revised form 3 May 2005; accepted 18 May 2005

Abstract

Environmental scanning electron microscopy (ESEM) enables wet samples to be observed without potentially damaging sample preparation through the use of partial water vapour pressure in the microscope specimen chamber. However, in the case of latices in colloidal state or microorganisms, samples are not only wet, but made of objects totally submerged in a liquid phase. In this case, under classical ESEM imaging conditions only the top surface of the liquid is imaged, with poor contrast, and possible drifting of objects.

The present paper describes experiments using a powerful new Scanning Transmission Electron Microscopy (STEM) imaging system, that allows transmission observations of wet samples in an ESEM. A special device, designed to observe all sorts of objects submerged in a liquid under annular dark-field imaging conditions, is described. Specific features of the device enable to avoid drifting of floating objects which occurs in the case of a large amount of water, thus allowing slow-scan high-definition imaging of particles with a diameter down to few tens of nm. The large potential applications of this new technique are then illustrated, including the imaging of different nano-objects in water. The particular case of grafted latex particles is discussed, showing that it is possible to observe details on their surface when submerged in water. All the examples demonstrate that images acquired in wet STEM mode show particularly good resolution and contrast, without adding enhancing contrast objects, and without staining.

© 2005 Elsevier B.V. All rights reserved.

Keywords: ESEM; Wet STEM; Water suspension; Nano-objects

1. Introduction

In conventional scanning electron microscopy (SEM) studies, the drastic drying conditions imposed by high vacuum in the microscope chamber have always prevented direct studies of

*Corresponding author. Groupe d'Etudes de Métallurgie Physique et de Physique des Matériaux, UMR CNRS 5510, INSA de Lyon, Bâtiment B. Pascal, 7 Avenue Jean Capelle, 69 621 Villeurbanne Cedex, France. Tel.: 00 33 4 72 43 61 30; fax: 00 33 4 72 43 85 28.

E-mail address: Agnes.Bogner@insa-lyon.fr (A. Bogner).

wet samples and dynamic imaging in a changing sample environment, as it is reported in Ref. [1]. For this reason, traditional microstructural characterization of delicate samples usually requires a preliminary preparation step, including fixing and staining. ESEM differs from a conventional SEM since the sample is not viewed under high vacuum. The column is divided into differential pressure zones that allows the electron gun to remain under high vacuum while the sample chamber contains a few torr of gas. Collisions between electrons and gas molecules produce positive ions that prevent the build-up of charges on insulating samples. This consequently eliminates the need for a conductive surface coating on insulators surfaces. Moreover, daughter electrons are produced thanks to a ‘cascade effect’ that amplifies the signal detected by the positively biased environmental detector. Eventually, when the microscope is equipped with a Peltier stage, the adjustable chamber pressure and temperature ranges enable the observation of wet samples in their natural state. For all these reasons, ESEM appears to be an ideal technique to study all kinds of wet nano-objects.

The observation of wet organic samples with ESEM has already been reported in the literature [1–3]. In all cases, special attention is recommended in order to minimize evaporation during the pump down sequence [4]. Then, the main difficulty that restricts observation during imaging is the fast sample damage under the incident electron beam. In the case of polymers, the degradation may be accelerated in the presence of water because of the high mobility of radicals through the water layer, which increases the rate of hydrolysis [2]. This prevents the successive imaging of the same area, and also limits the imaging magnification—higher magnification means higher irradiation dose and therefore more damage. Finally, one should keep in mind that only the top layer of the sample surface is revealed, which means that classical use of ESEM does not allow the observation of samples deep inside the liquid layer.

This paper presents, a new “wet STEM” device developed for the transmission imaging of suspensions—i.e. objects from a few nm to several μm stabilized in a liquid phase, latices (in polymer

science terminology, latex means a colloidal suspension of polymer particles in an aqueous solution) or emulsions (droplets of liquid dispersed in another liquid phase). Thanks to its development in an ESEM, it is a straight-forward analysis technique. Its application is illustrated through several cases: organic and inorganic objects, monomer and polymer emulsions. For sake of clarity in the experimental description, the term “suspension” is used for all the samples imaged.

2. Experimental device

The observations have been performed with a FEI XL 30 FEG ESEM. The specific device developed for imaging wet samples in transmission mode, and hereafter called “wet STEM”, is described in Fig. 1.

2.1. Experimental setup

A TEM copper grid is placed on the head of a TEM sample holder, which is fixed on a round

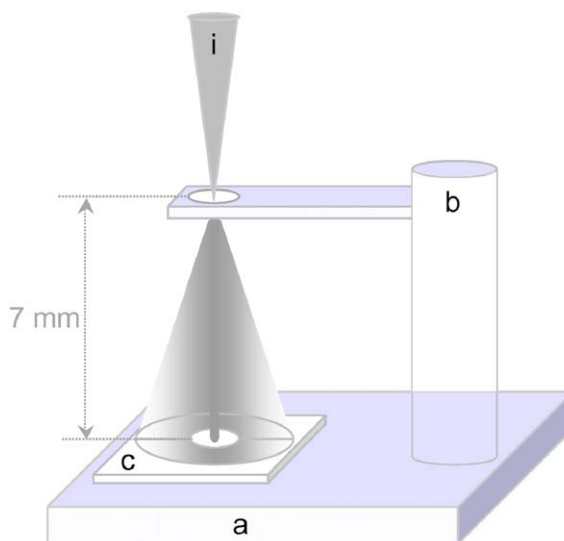


Fig. 1. Schematic of the wet STEM device for annular dark-field imaging. (a) Peltier stage, (b) SEM mount supporting the latex droplet on a TEM grid, (c) solid-state detector, usually used for the collection of BSE, removed from its position and located below the specimen and (i) Convergent incident beam. Remark: the direct transmitted beam is not collected.

cylindrical SEM mount, and positioned on the Peltier stage. A droplet of liquid containing particles or floating objects (organic, inorganic, liquid or solid) is dropped on the grid with an eppendorf[®] micropipette. In these conditions, the incident electron beam passes through the droplet, i.e. the liquid layer and a given amount of floating particles. The signal is then collected by a detector, usually used for the collection of backscattered electrons (BSE), but in our case located below the sample. We used holey carbon coated TEM copper grids, with the carbon layer down in order to use copper squares as retention basins. In the carbon layer, holes of typical diameter ranging from less than 1 to 20 μm allow maintaining overhanging liquid films on very small areas. It is important to note that adequate initial droplet parameters—i.e. volume and solid content—enable to control the amount of particles on the grid. It is possible, for instance in the case of a latex emulsion sample, to choose to image only a monolayer of particles if required.

Due to the initial concentration of the suspension, when the droplet of smallest volume that can be dropped contains more objects than for a monolayer on the grid, a dilution step with distilled water can be performed.

Classical ESEM detectors also available enable the control of the sample surface in SE mode and in BSE mode, using the gaseous SE detector GSED, and the gaseous backscattered electron detector GAD, respectively. This is very helpful for example to control the presence of liquid until the thickness is adequate to perform transmission observations and to detect if objects are not submerged in water anymore.

2.2. Purge sequence

In relation with the work described in Ref. [4], an optimized pump down sequence is used in order to prevent evaporation from, and condensation on the sample droplet. Parameters like water source bottle temperature, sample temperature, initial relative humidity rate in the microscope chamber, number of pumping and flooding cycles, upper and lower pressures for the purge are carefully controlled during the sequence.

2.3. Imaging sequence

The pressure and temperature can be adjusted to evaporate a small amount of water from the droplet. It allows to keep a water layer thin enough so that electrons both transmitted and scattered pass through it, and can be collected to participate to the formation of a STEM image. Thin films of wet samples are created in situ in the ESEM chamber, their thickness depending on the quantity of water evaporated from the initial droplet. The solid content of the sample is controlled so that the initial solid content and the initial droplet volume are known. As evaporation is an endothermic reaction, it is then possible to follow it by checking the difference between the setting temperature and the measured one. Then the thickness of the film is kept constant thanks to an equilibrium water pressure using the (P,T) water diagram [5]. For instance, a water pressure of 5.3 torr is required at a sample temperature of 2 °C, so that objects remain in a constant water layer. By controlling the sample temperature through the Peltier stage, and using water vapour as the imaging gas at a controlled pressure, samples can be kept above their saturated vapour pressure during all the experiment.

2.4. Imaging mode

In SEM, the detection strategy in STEM mode is based on the direct collection of electrons passing through the sample, by a solid-state detector (two semi-annular detectors A and B). For the configuration usually used, the incident electron beam arrives on the limit of diodes A and B, and bright- or dark-field images can be produced with the collection of transmitted or scattered electrons, respectively. In this case, only a small area of the sample is above the limit of A and B. In the present study, we choose another possibility: annular dark-field imaging conditions can be obtained if the dipolar detector is placed so that it occults the transmitted electron beam and it only collects scattered beams on a ring constituted by both diodes A and B. Using this method, a more important part of the scattered electrons available is used to form an image and more

contrasted images can be obtained. Consequently, all the ESEM micrographs presented in the following have been obtained in annular dark-field conditions. The second advantage of this disposition, using the sum signal, is that imaging conditions are not linked to the area of the sample imaged.

Moreover, in our experimental setup, the distance between the sample and the detector has been investigated in order to optimize the contrast. Best results are obtained with a distance of about 7 mm, corresponding to collection angles between 20° and 45° in dark field. However, this optimum is empirical. Its theoretical explanation is complex due to the different diffusion mechanisms involved in images formation, and is not in the frame of this study.

3. Applications of the wet STEM mode for imaging nano-objects in water

3.1. Applications to a large pallet of samples

In order to highlight the wide variety of imaging possibilities in wet STEM, different samples have been observed in this mode.

For an evaluation of the resolution reached in wet STEM mode, gold nano-particles in colloidal solution have been observed in wet STEM. The synthesis process of these suspensions is described in Ref. [6]. Fig. 2 presents a comparison between SE mode, backscattered electron mode and wet STEM images. SE imaging in wet mode (Fig. 2a) does not allow to observe any details except the surface of the water layer. Fig. 2b has been acquired using BSE: a very good contrast is obtained, thanks to the high atomic number difference between the Au particles and the liquid water, allowing Au particles network to be imaged. In wet STEM mode (Fig. 2c), even with a large thickness of water, Au particles are also detected. When the water layer thickness decreases (Fig. 3), the wet STEM image is better than the BSE image, and gives access to individual visualization of each particle. The mean particle size is around 20 nm, and the resolution reaches 5 nm, an

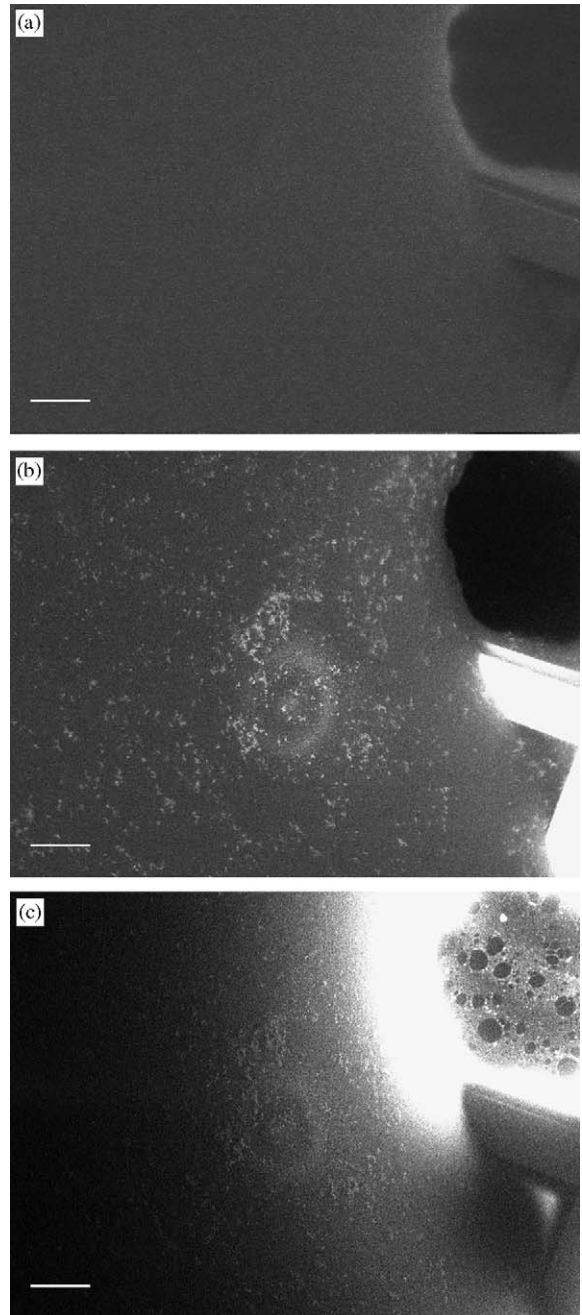


Fig. 2. Colloidal solution of gold nano-particles, imaged at 30 kV in wet mode with different electron detectors: (a) large field gaseous SE detector (GSED), (b) gaseous backscattered electron detector (GAD) and (c) annular dark-field STEM detector. Scale bar length: 25 μm .

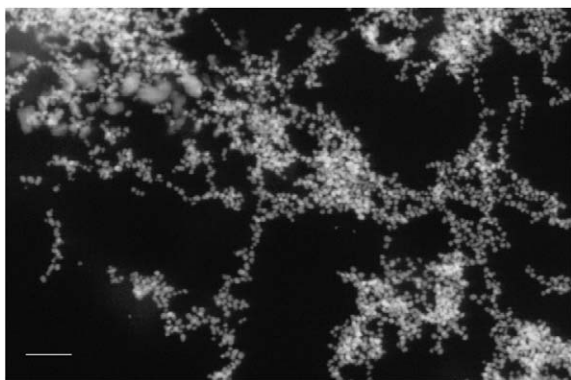


Fig. 3. Colloidal solution of gold nano-particles imaged at 30 kV in wet mode with the annular dark-field STEM detector. Average particles size: 20 nm. Scale bar length: 200 nm.

excellent result partly thanks to the field emission source.

Particles with similar sizes but with a less favourable atomic number difference with water have then been chosen to evaluate wet STEM performances. A colloidal suspension of silica particles, supplied by Buehler under the commercial name Mastermet[®]2, has been observed. Referring to the commercial catalogue, monodisperse particles with a size around 20 nm were expected. Fig. 4 shows two images at different magnifications, *15,000 and *120,000, respectively. On the first image, the large several μm -wide circle is a hole in the carbon layer of the TEM grid. Wet STEM images show a wide dispersion in particle sizes, ranging from 20 to 100 nm. Above the carbon grid hole, a water meniscus has been formed, so that biggest particles have been rejected on edges, where the water layer is thicker. On every point of the hole area, as the water layer is just slightly thicker than the particles and the Z number of particles is greater than that of water, one can observe a classical dark field contrast, i.e. larger particles appear brighter.

From these examples, one can see that metallic and inorganic nano-objects in water observed in wet STEM exhibit interesting resolution and contrast. The following example concerns organic nano-objects: multi-walls carbon nanotubes, dispersed in water [7]. Wet STEM image on Fig. 5 is

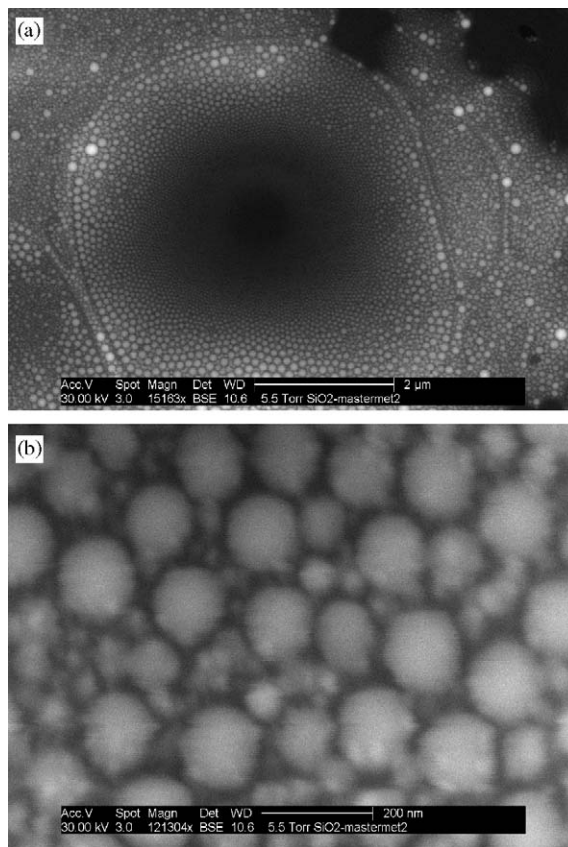


Fig. 4. Colloidal solution of silica particles (polishing product Mastermet 2 supplied by Buehler) imaged at 30 kV in wet mode in annular dark-field conditions. Particles size ranges from 20 to 100 nm.

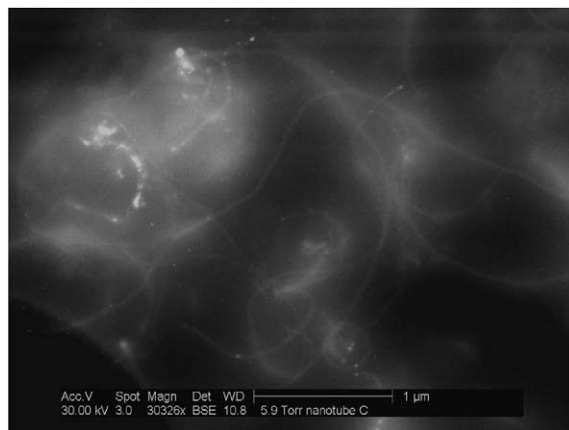


Fig. 5. Carbon nanotubes in water imaged at 30 kV in wet mode in annular dark-field conditions.

well contrasted and helps for the understanding of nanotube conformations i.e. the positions they adopt in volume. It is specially interesting because this information should not be very different from the conformation of nanotubes mixed in a latex suspension, which is used to synthesize polymer films with fillers inducing specific electrical properties.

In the present wet STEM imaging mode, signal detection conditions have been optimized, in order to obtain strong contrasts thanks to annular dark-field conditions. This is specially interesting for polymer and biological samples, known to give low contrasts because of their low atomic numbers. Wet STEM observations are performed in a water layer that is to say in the actual environment of the samples, and in all cases, the individual particles are well resolved. But another experiment allowed with the present STEM device is the use of ESEM ability for dynamic imaging. A synthetic latex has been observed during in situ water evaporation. The STEM image presented on Fig. 6 shows a pile-up of particle layers, that means that multi-layers are detected in this mode.

We turn now to observe more delicate samples i.e. a liquid–liquid suspension, constituted with an aqueous phase including organic liquid spheres

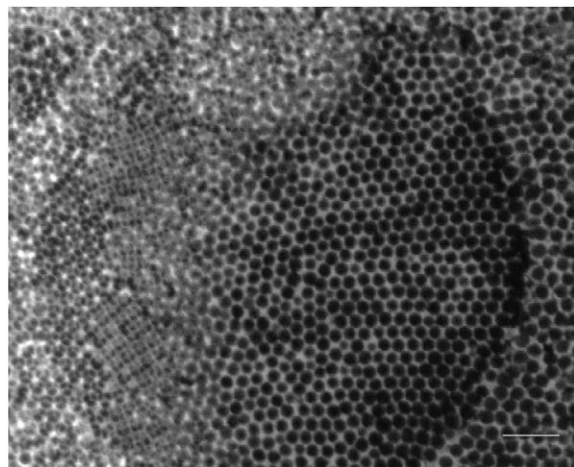


Fig. 6. Deformed particles of homogeneous acrylic latex during evaporation by heating: on the right, a monolayer, and on the left, a pile-up of particles layers. The large circle is a hole in the carbon layer of the TEM grid. Scale bar length: 500 nm.

stabilized by a surfactant. These samples are made from mini-emulsion polymerization technique, which can be employed to synthesize high solid content latices. During polymerization, floating objects included into water are evolving from monomer droplets to solid polymer particles. Using the present wet STEM imaging system, two mini-emulsions have been characterized, corresponding to two different stages of the polymerization process. Fig. 7 presents wet STEM: a mini-emulsion of styrene in water (Fig. 7a), and an hybrid mini-emulsion of polystyrene–styrene in water (Fig. 7b). With the help of classical image analysis (SIS software), we found that monomer droplets sizes range from 150 to 400 nm and are homogeneously distributed. On the same figure, it

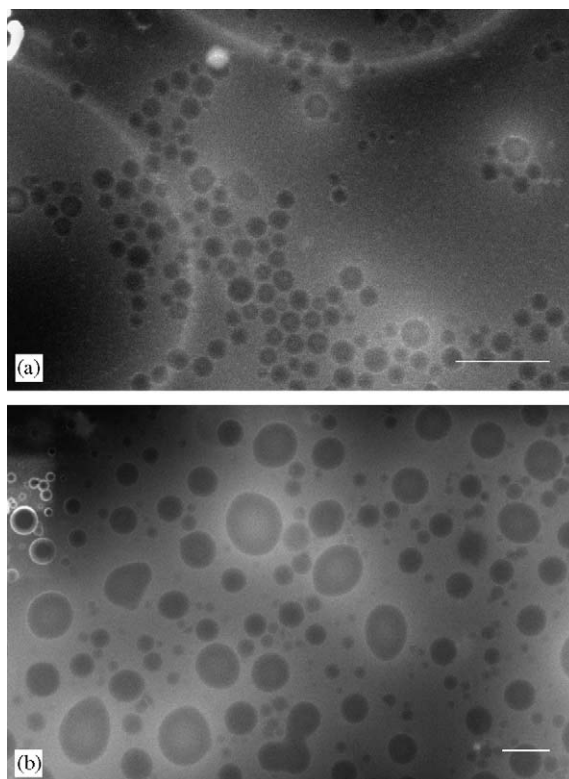


Fig. 7. Wet STEM images at 30 kV in annular dark-field conditions of aqueous mini-emulsions of (a) styrene in water, (b) polystyrene–styrene in water. Larger circles of several μm diameter are holes in the carbon layer of the TEM grid. Scale bar length: 1 μm .

is again possible to distinguish two large circular lines with radius higher than several μm , corresponding to hole edges in the carbon layer of the TEM grid. For hybrid styrene–polystyrene mini-emulsion, droplets have sizes ranging from 90 to 900 nm and droplet size distribution (DSD) is very large, the main part being between 200 and 300 nm. The accuracy of these values have been confirmed after microscope calibration for the magnifications used. As a remark about image in Fig. 7b, a brighter area can be observed on the left corner of the micrograph. This is the result of the preliminary imaging of this area at higher magnification, where electron beam is assumed to produce charging effects. The huge interest of this technique in the specific field of mini-emulsion is commented in Ref. [8]. If the sample dilution and the imaging magnification are adequate, it allows to determine both average droplet size and DSD, which directly influence the mini-emulsion stability and the nucleation mechanism.

These examples show that the wet STEM method is particularly adapted to image nano-objects (metallic, inorganic, organic, liquid) in a water layer. It gives access to size and size distribution, and can also be used to determine the stability of objects in the liquid phase.

3.2. Application for the imaging of grafted colloidal aqueous latices

Wet STEM is also a very powerful analysis method to detect details on the surface of nano-objects included in a liquid phase. An example is presented in this section, where natural rubber latex particles are imaged before and after grafting on their surface.

In its native state, natural rubber is a poly-disperse latex and in the present latex *Hevea Brasiliensis*, particles sizes range from 40 nm to 3 μm . Natural rubber shows excellent properties such as high resilience, strength, and fatigue resistance, but most of its industrial applications require the addition of reinforcing fillers like carbon black or silica, in order to increase the modulus and the wear resistance. In the case of silica fillers, a good dispersion of the particles can be obtained using two methods: (1) by fillers

surface modification, or (2) by chemical modification of the natural rubber itself. Different morphologies of the chemically modified particles are thus obtained: core-shell type, inverted nucleus, raspberry-like, fruit cake and hairy-layer. In order to improve its affinity with silica, use is made of hydrophilic polymer chains, and the process is optimized so that the hydrophilic chains are grafted on the particle surface, i.e. the morphology should be either core-shell type or hairy-layer type [9]. This last solution can be carried out by the grafting of a hydrophilic polymer poly(DMAEMA) on the natural rubber latex particles by seeded emulsion polymerization. Gilbert et al. [10] have reported that this grafting results in a copolymer acting as electrosteric stabilizer. The DMAEMA monomer is indeed a tertiary amine that can be protonated in acid conditions. In this way, although the modified latex displays a poor colloidal stability at $\text{pH} \approx 8$, it shows a drastic improvement in colloidal stability in acid conditions ($\text{pH} = 2$), attributed to the electrosteric stabilizer role of the grafted hydrophilic polymer. Wet STEM observations are used to study directly grafted hairy-layer particles of natural rubber latices in acid conditions and to compare them with non-grafted natural rubber latex particles.

Figs. 8 and 9 show a comparison between wet STEM images and ultramicrotomy sections observed in STEM mode for non-grafted natural rubber (NR) particles and NR particles grafted with poly(DMAEMA) respectively. As expected, the particles size distribution is polydisperse with sizes ranging from several tens of nm to 3 μm .

First, the geometrical stability of non-grafted particles (Fig. 8) seems lower than that of grafted ones (Fig. 9). Some particles show deformations and look more oval than spherical. This observation confirms the assumed stabilizing role of the grafting.

Secondly, the texture and contrast of the particles surface imaged differ totally in the case of grafted latices in comparison with non-grafted ones. Indeed, non-grafted particles surface seems very smooth, whereas grafted particles present a granular surface texture. This difference in particles surface aspect is related to the homogeneous particles morphology of non-grafted particle and

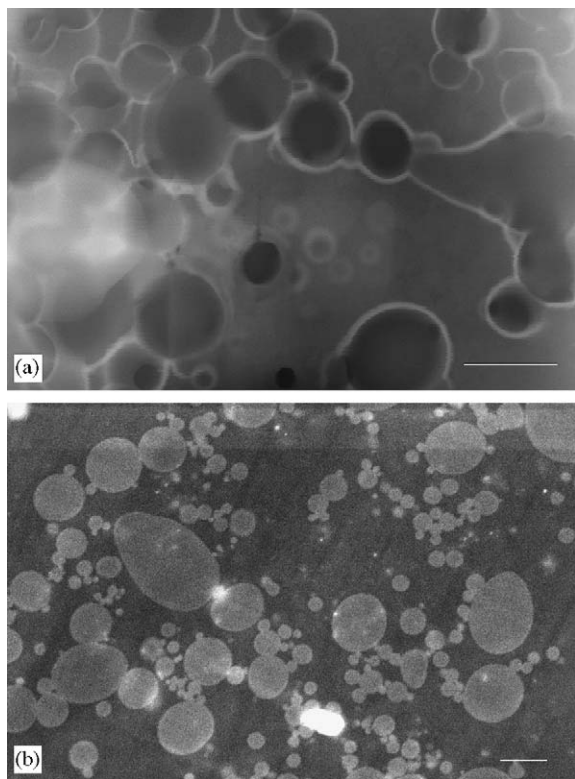


Fig. 8. Natural rubber latex (NRL): (a) droplet imaged at 30 kV in annular dark-field wet STEM conditions *without staining or other preparation*: pure NRL, (b) ultramicrotomy foils encapsulated in a resin and imaged at 30 kV in annular dark-field STEM conditions. Scale bar length: 1 μm .

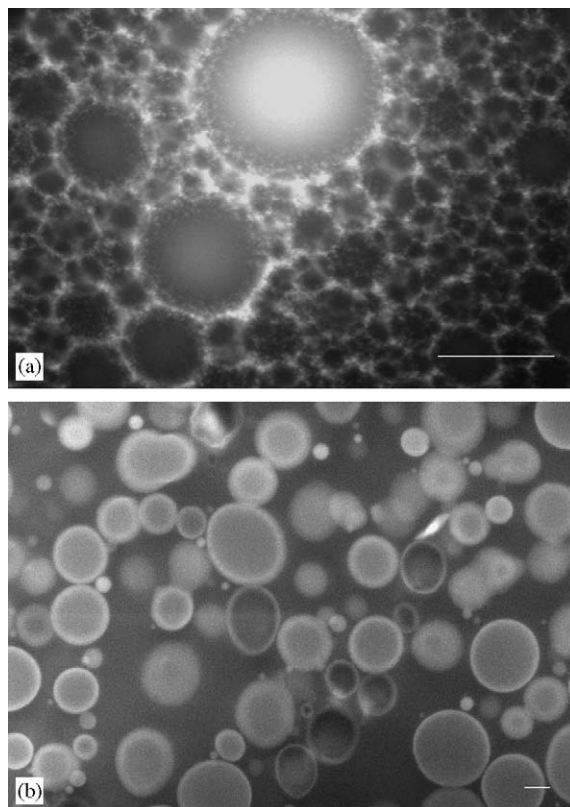


Fig. 9. Natural rubber latex (NRL) grafted with poly(DMAEMA): hairy-layer morphology: (a) droplet imaged at 30 kV in annular dark-field wet STEM conditions *without staining or other preparation*, (b) ultramicrotomy foils encapsulated in a resin, and imaged at 30 kV in annular dark-field STEM conditions. Scale bar length: 500 nm.

to the hairy-layer morphology of poly DMAEMA grafted particles.

In addition, if the size distribution of particles is very large for both of the latices, their average size seems to change with grafting. Non-grafted particles exhibit slightly smaller diameters than grafted ones. These observations confirm the results obtained by dynamic light scattering measurements performed with a Beckman Coulter apparatus, Mod. LS230: a mean diameter of 170 nm is obtained for non-grafted particles and of 210 nm for particles grafted with poly DMAEMA.

The comparison between wet STEM images and STEM images of foils prepared by ultramicrotomy is quite interesting. Both are precious for the characterization of morphologies resulting from

grafting. But there is an important difference between these samples in the time required for preparation, since wet STEM does not require any. Although no staining has been performed on samples imaged in wet STEM mode, the resulting contrast is greater. It should be noted that wet STEM contrast of particles differs from STEM images of ultramicrotomed foils. In the first case, we pass through a whole particle (edges thinner, i.e. darker than centre), whereas in the second case, only a slice of particle is imaged (one grey level). At last, the comparative study constitutes a good validation of the wet STEM techniques.

It can be noted that wet STEM imaging brings a new and direct method for the puzzling task of

grafting characterization, for which no other direct determination is available. Wet STEM observations are very reproducible and allow to highlight many differences in particles aspect between the two different latex samples.

3.3. Prospects

For prospective evaluation, two samples very different from the applications described in previous sections have been imaged in annular dark field wet STEM conditions.

Firstly, a suspension-type sample where the liquid phase is not water, is presented on Fig. 10. The STEM image shows details of a very thin motor oil layer slightly diluted in hexane, and deposited on a TEM grid. Soot particles resulting from incomplete combustion and arranged in a quasi-percolating network, partially broken during the dilution step, have been imaged with good contrast and resolution. These results encourage future characterization of nano-objects in wet STEM mode, varying the nature of the liquid layer, provided that pressure and temperature ranges available in ESEM allow maintaining the sample above its saturated vapour pressure.

Secondly, biological samples included in water have been imaged in wet STEM mode. These samples are particularly sensitive to dehydration

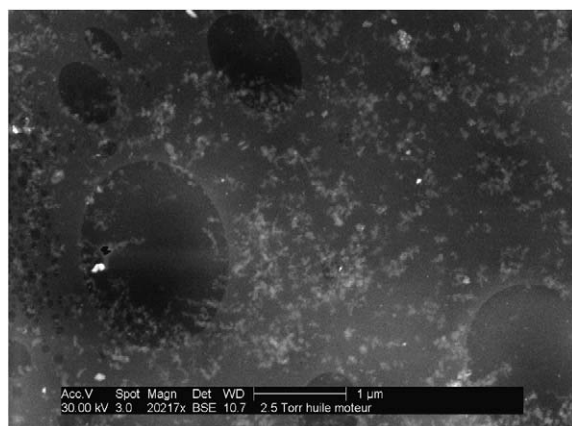


Fig. 10. Annular dark-field wet STEM image at 30kV of organic objects submerged in a liquid phase: motor-oil containing soot particles arranged in a percolating network.



Fig. 11. Annular dark-field wet STEM image at 30kV of organic objects submerged in a liquid phase: *Pseudomonas syringae* pv. *Syringae* bacteria, strain PPI203: double membrane structure and cellular division are observed.

and beam damage. Fig. 11 shows bacteria of the species *Pseudomonas syringae*, where different steps of cellular division are observed. Thanks to transmission mode, details like double membrane structure are also well distinguished in wet STEM, in comparison with classical ESEM imaging. The wet STEM imaging mode appears to be a straightforward and powerful imaging for two reasons: first, no staining preparation is required to obtain high contrast even with low atomic number elements; second, the native state of the sample, i.e. the hydrated state, can be imaged, since no sample preparation is required previously.

Of course, the ability of ESEM to control evaporation through temperature and pressure variations allow to envisage the imaging of in situ evolutions of suspension-type samples: film-forming process in latices.

4. Discussions about wet STEM imaging mode

As presented in the Section 3, wet STEM allows observing directly a liquid layer containing nano-objects, partially thanks to its development in SEM, in addition in Environmental SEM. Firstly, wet environment and possibility of dynamic imaging are specific to ESEM, and constitute a

part of the interest of wet STEM. The specimens can indeed be maintained in their wet state, so that particles included in a layer of liquid are imaged. In this way, they are neither deformed nor collapsed, and their size can be correctly estimated. If required, their dynamic evolution can also be followed in situ, when evaporation occurs for example. Secondly, the quite low voltages used in SEM (1–30 kV) in comparison with TEM give access to a higher number of electrons–sample interactions, resulting in more contrasted images [11]. Finally, thanks to the development of field emission guns [12], the resolution available in SEM is now appreciable, so that SEM imaging becomes an easy characterization method with a very high resolution, reaching 1 nm in STEM mode at an acceleration voltage of 20 kV. Thanks to the field emission gun, nano-particles or objects around 20 nm can easily be imaged in wet STEM mode, where the resolution has experimentally been shown to be lower than 5 nm (colloidal solution of Au particles).

Another interest of the wet STEM mode in ESEM is the fact that it brings a new pallet of imaging possibilities. Indeed, in the case of nano-objects included in a liquid, classical ESEM imaging shows some limits. A characteristic of wet STEM imaging method vs. classical ESEM, thanks to transmission mode, is the access to volume information in a liquid. As we image the entire volume of the liquid, we observe not only the smooth surface of the colloidal solution or some particles emerging from this liquid phase, but also objects deep inside a liquid layer, and the way particles are piled up, whilst being limited by electrons transmission. Areas of particles layers superposition can also be detected and imaged.

Images interpretation sometimes leads to questions, and it is still difficult to explain every contrasts theoretically because of the complexity of the numerous diffusion mechanisms involved in images formation. This aspect still needs further investigation, through the development of Monte Carlo simulation. However, it is already possible to state some remarks about the colloidal solutions imaged. Particles imaged in this mode usually exhibit a halo or brighter contrast around the

particle. In annular dark-field conditions, the contrast can be described as a mass–thickness inverse type [13]. As a result, brighter contrasts are interpreted as thicker or higher atomic number composition areas. In this way, biggest particles look brighter, and light their environment so that a large area around big particles looks brighter, and the halo effect is enhanced for each particle. In addition, particles in colloidal state are often stabilized thanks to ionic surfactants. The presence of these negative charges may interact with diffused electrons and participate to create a halo around particles.

In a TEM, high collection angles are not used because the signal would suffer from lens aberrations. Other benefits occur in our case, thanks to SEM characteristics: high angles can be used for collection resulting in an increased signal level [12,14] and low voltages available induce an improved contrast.

Wet STEM requires thin samples in order to obtain an important transmission signal. In the case of colloidal solutions, this low thickness eliminates the usual drift phenomenon always occurring on large size drops, which prevents imaging even with high scanning rate acquisition. Liquid is indeed maintained on small areas defined by the TEM grid, through copper squares and holes in the carbon layer. These small areas can be observed using slow scan imaging conditions, known to increase image quality especially in environmental mode.

Polymers or other organic objects are very high damage-sensitive samples, moreover, in the presence of water [15], and are not adapted to several imaging of a given area. However, damage effects can be reduced by using low-dose methods [16]. Focus, astigmatism and wobblers readjustments are done away from the image, the beam then being moved on the area of interest just for the acquisition. The aim is to prevent beam damage on the area prior to the image recording. This minimizes the exposure time and the cumulated dose. In addition, as a compromise between contrast and damage, the maximum acceleration tension has been used (30 kV), because higher tension means lower electron–sample interactions [11].

In addition, the low thickness of our samples also induces a smaller interaction volume in comparison with classical SEM samples, which also means a smaller damaged volume. Most of the beam passes through, resulting in transmitted and scattered beam [14]. Moreover, in the case of sub-micrometric particles examination in conventional SEM, specially those composed of low atomic number elements, the electron beam penetrates the entire particle and the substrate below—the interaction volume is greater than the particles—in such a way that the signal quality is affected [17]. Using STEM imaging, where the specimen is changed from a bulk material to a thin film supported by a grid, detection and visualization of particles are improved, and image quality increases.

5. Conclusions

The present wet STEM imaging system, new toolkit developed in ESEM, allows straightforward transmission observations of wet samples constituted by nano-objects included in a water layer. A specially good resolution can be achieved: 5 nm with a kind of resolution testing sample: gold nano-particles colloidal suspensions. The contrast is enhanced thanks to low voltages, and annular dark-field imaging conditions, specially interesting for low atomic number materials. This transmission technique gives access to volume information so that we do not image only the surface of the water drop. It helps to limit drifting phenomenon of objects floating in a large amount of water, so that it allows slow-scan high-definition imaging. The main limits that make the imaging sequence more delicate are beam damage effects, enhanced in the presence of water.

The huge interest of the present imaging method in the specific field of suspensions is highlighted in this paper. The size and size distribution of nano-objects are easily determined, and suspension stability can be evaluated. In addition, even if complete image interpretation needs further investigations, contrast is well understood, and thin details can be detected on suspended nano-objects, as shown in the case of latex grafted particles.

Comparative approach between wet STEM images and others observations and characterization results are very interesting. Comparison between different samples also bring a lot of precious information about samples.

Acknowledgements

We wish to thank all the samples suppliers: A. and R. Guimarães (GEMPPM and Dequi-Faenquil—Lorena, Brazil) for natural rubber latices, J. M. Asua, (Institute for Polymer Materials—San Sebastian, Spain) for mini-emulsions, F. Dalmas (GEMPPM) for carbon nanotubes, P. Oger (LST—ENS Lyon) for *Pseudomonas syringae* bacteria, S. Roux (LPCML—UCB Lyon 1) and P. Perriat (GEMPPM) for gold nano-particles suspensions. We present our special acknowledgements to K. Masenelli-Varlot (GEMPPM) for ultramicrotomed foils preparation.

The Consortium Lyonnais de Microscopie Electronique is thanked for the access to the FEI XL 30 FEG ESEM.

This work was financially supported by Total France S. A.

References

- [1] J.L. Keddie, P. Meredith, R.A.L. Jones, A.M. Donald, *Macromol.* 28 (1995) 2673–2682.
- [2] A.M. Donald, C.B. He, C.P. Royall, M. Sferrazza, N.A. Stelmashenko, B.L. Thiel, *Colloids Surf. A* 174 (2000) 37–53.
- [3] D.J. Stokes, *Adv. Eng. Mater.* 3 3 (2001) 126–130.
- [4] R.E. Cameron, A.M. Donald, *J. Microsc.* 173 (1994) 227–237.
- [5] A.M. Donald, *Nat. Mater.* 2 (2003) 511–516.
- [6] S.M. Chabane Sari, P.J. Debouttière, R. Lamartine, F. Vocanson, C. Dujardin, G. Ledoux, S. Roux, O. Tillement, P. Perriat, *J. Mater. Chem.* 14 (2004) 402–407.
- [7] F. Dalmas, L. Chazeau, C. Gauthier, K. Masenelli-Varlot, R. Dendievel, J.-Y. Cavailé, L. Forro, *J. Polym. Sci. Part B : Polym. Phys.* 43 (2005) 1186–1197.
- [8] M. do Amaral, A. Bogner, C. Gauthier, P.-H. Jouneau, J.M. Asua, G. Thollet, *Macromol. Rapid Commun.* 26 (2005) 365–368.
- [9] P.C. Oliveira, A. Guimarães, J.-Y. Cavailé, L. Chazeau, R.G. Gilbert, A.M. Santos, *Polymer* 46–4 (2005) 1105–1111.

- [10] D.J. Lamb, J.F. Anstey, C.M. Fellows, M.J. Monteiro, R.G. Gilbert, *Biomacromol.* 2 (2001) 518–525.
- [11] D.B. Williams, C.B. Carter, *Transmission Electron Microscopy—III. Imaging*, Plenum Press, New York.
- [12] L. Reimer, *Scanning Electron Microscopy: Physics of Image Formation and Microanalysis*, second ed, Springer, Berlin, Heidelberg, New York, 1998.
- [13] C.J.G. Plummer, EPFL, *Techniques de l'ingénieur AM 3 282*
- [14] L.C. Sawyer, D.T. Grubb, *Polymer Microscopy*, Chapman and Hall, London, 1987.
- [15] S. Kitching, A.M. Donald, *J. Microsc.* 190 (1998) 357–365.
- [16] K. Varlot, Ph.D. Thesis, Ecole Centrale de Lyon, 1998.
- [17] J. Goldstein, et al., *Scanning Electron Microscopy and X-ray Microanalysis*, second ed, Plenum Press, New York, 1992.